Behavioral/Systems/Cognitive

Phospholipase C β4 in the Medial Septum Controls Cholinergic Theta Oscillations and Anxiety Behaviors

Jonghan Shin,[1,2] Gangadharan Gireesh,[2] Seong-Wook Kim,[2,3] Duk-Soo Kim,[2] Sukyung Lee,[4] Yeon-Soo Kim,[4] Masahiko Watanabe,[5] and Hee-Sup Shin[2]

[1]Neuroscience Research Institute, Gachon University of Medicine and Science, Incheon 405-760, Republic of Korea, [2]Center for Neural Science, Korea Institute of Science and Technology, Seoul 136-791, Republic of Korea, [3]Neuroscience Program, University of Science and Technology, Daejon 305-333, Republic of Korea, [4]Department of Smart Foods and Drugs and Indang Institute of Molecular Biology, Inje University, Seoul 100-032, Republic of Korea, and [5]Department of Anatomy, Hokkaido University School of Medicine, Sapporo 060-8638, Japan

Anxiety is among the most prevalent and costly diseases of the CNS, but its underlying mechanisms are not fully understood. Although attenuated theta rhythms have been observed in human subjects with increased anxiety, no study has been done on the possible physiological link between these two manifestations. We found that the mutant mouse for phospholipase C β4 (PLC-$\beta4^{-/-}$) showed attenuated theta rhythm and increased anxiety, presenting the first animal model for the human condition. PLC-β4 is abundantly expressed in the medial septum, a region implicated in anxiety behavior. RNA interference-mediated PLC-β4 knockdown in the medial septum produced a phenotype similar to that of PLC-$\beta4^{-/-}$ mice. Furthermore, increasing cholinergic signaling by administering an acetylcholinesterase inhibitor cured the anomalies in both cholinergic theta rhythm and anxiety behavior observed in PLC-$\beta4^{-/-}$ mice. These findings suggest that (1) PLC-β4 in the medial septum is involved in controlling cholinergic theta oscillation and (2) cholinergic theta rhythm plays a critical role in suppressing anxiety. We propose that defining the cholinergic theta rhythm profile may provide guidance in subtyping anxiety disorders in humans for more effective diagnosis and treatments.

Introduction

Anxiety is both a normal emotion and a psychiatric disorder. Anxiety disorders lead to profound suffering and disability that can markedly disrupt family life as well as the life of the sufferer, especially when associated with avoidance behavior and agoraphobia (Gray and McNaughton, 2000; Nutt, 2005; Kim et al., 2010). Although attenuated theta rhythms have been observed in human subjects with increased anxiety (Mizuki et al., 1989; Suetsugi et al., 2000), this phenomenon has not been replicated in animal models of anxiety disorders (Mitchell et al., 2008). Instead, in rodent models of anxiety, it has been shown that (1) GABAergic and serotonergic anxiolytic drugs reduced the frequency of hippocampal theta rhythms elicited by brainstem stimulation (McNaughton et al., 2007), whereas cholinergic drugs did not (Kinney et al., 1999); and (2) increased hippocampal theta rhythms, generated during locomotion in the serotonergic receptor $5HT_{1A}$ knock-out mice, showed a positive correlation with an increased anxiety level (Gordon et al., 2005).

Interestingly, the heterogeneity of hippocampal rhythmic oscillatory activities at the theta frequency (4–12 Hz) has been associated with cholinergic, GABAergic, or serotonergic transmission (Bland, 1986; Leung, 1998; Buzsáki, 2002; Shin et al., 2005). For example, (1) the muscarinic acetylcholine receptor(s)–phospholipase C β1 signaling pathway underlies cholinergic theta rhythms generated in some behavioral conditions such as undisturbed urethane anesthesia, alert immobility, and passive whole-body rotation (Shin, 2002, 2009; Shin et al., 2005); (2) hippocampal theta rhythms generated during locomotion was strongly reduced in genetically modified mice in which synaptic inhibition was ablated in parvalbumin (PV)-positive GABAergic interneurons (Wulff et al., 2009); and (3) hippocampal theta rhythms generated during locomotion was increased in the serotonergic $5HT_{1A}$ knock-out mice (Gordon et al., 2005). Therefore, the theta rhythm heterogeneity appears to be associated with different biochemical and behavioral conditions, and may provide an insight into understanding the heterogeneity of anxiety disorders.

Phospholipase C β (PLC-β) isozymes represent a family of molecules that link GPCRs (G-protein-coupled receptors) to an intracellular signaling network (Hwang et al., 2005). PLC-β4, one of the four PLC-β isoforms (PLC-β1, PLC-β2, PLC-β3, and PLC-β4), is activated via the metabotropic glutamate receptor 1α (mGluR1a) and is predominantly expressed in the soma and dendrites of neurons in the medial septum (Watanabe et al., 1998; Nakamura et al., 2004), one of the three brain regions (hippocampus, amygdala, and septum) implicated in anxiety behaviors (Treit and Menard, 1997; Gray and McNaughton, 2000). The medial septum is also a nodal point involved in generating hippocampal theta rhythms (Bland, 1986; Leung, 1998; Buzsáki, 2002). These observations present a possibility that PLC-β4 may

Received July 1, 2009; revised Oct. 4, 2009; accepted Oct. 9, 2009.

This work was supported by 21C Frontier Proteomics Program of the Ministry of Education, Science and Technology (Korea), the National Honor Scientist Program of Korea, and the Center of Excellence Program of the Korea Institute of Science and Technology. We thank Yoon-Young Park and Sangmi Han for technical assistance.

Correspondence should be addressed to Hee-Sup Shin, Center for Neural Science, Korea Institute of Science and Technology, 39-1 Hawolgok-dong, Seongbuk-ku, Seoul 136-791, Republic of Korea. E-mail: shin@kist.re.kr.

DOI:10.1523/JNEUROSCI.3126-09.2009

 0270-6474/09/2915375-11$15.00/0

be critically involved in linking anxiety behaviors and theta rhythm heterogeneity.

We have tested this possibility by analyzing PLC-β4-knockout (PLC-$\beta4^{-/-}$) mice. The results show that a global deletion or a medial septum-selective knockdown of PLC-β4 attenuated cholinergic theta rhythms and increased anxiety behaviors in the mouse. Furthermore, a treatment with rivastigmine, a drug known to increase acetylcholine levels in the hippocampus, cured cholinergic theta rhythm anomalies and anxiety behaviors in PLC-$\beta4^{-/-}$ mice. These results reveal a critical role of PLC-β4 in the relationship between anxiety behaviors and cholinergic theta rhythms, and suggest that measuring cholinergic theta rhythms can provide effective guidance for subtyping anxiety disorders for optimal therapeutic benefit.

Materials and Methods

PLC-β4-null (PLC-$\beta4^{-/-}$) mutant animals. F_1 homozygous mice and wild-type (WT) littermates were obtained by crossing C57BL/6J(N8)PLC-$\beta4^{+/-}$ and 129S4/SvJae(N8)PLC-$\beta4^{+/-}$ mice. The genotypes were determined using PCR analyses as described previously (Kim et al., 1997). Animal care and handling procedures followed institutional guidelines (Korea Institute of Science and Technology, Seoul, Korea). Mice were maintained with *ad libitum* access to food and water under a 12 h light/dark cycle with light beginning at 6:00 A.M.

Production of lentiviral vectors. Lentiviruses were produced by cotransfecting HEK293T cells with three plasmids: (1) a construct expressing the heterologous envelope protein, VSV-G (vesicular stomatitis virus G); (2) a packaging-defective helper construct expressing the *gag-pol* gene; and (3) a transfer vector harboring a PLC-β4-specific short hairpin RNA (shRNA) sequence. Cells were transfected using Lipofectamine Plus as described by the manufacturer (Invitrogen). Forty-eight hours after transfection, virus-containing culture supernatants were collected, clarified by passing through a 0.45 μm membrane filter (Nalgene), and stored immediately at −70°C. Titers were determined using a p24 ELISA (PerkinElmer Life Science) or by Western blot analysis using a monoclonal anti-p24 antibody obtained through the AIDS Research and Reference Reagent Program. The titer of our preparations was routinely $\sim10^6$–10^7 transduction units (TU)/ml before concentration. Infectious lentivirus particles were concentrated by ultracentrifugation on a 20% sucrose cushion (2 h at 50,000 × *g*) at 4°C. Finally, titer of lentivirus for *in vivo* injection was 10^7 TU/μl.

shRNA expression and verification of shRNA-mediated knockdown of PLC-β4. PLC-β4-specific and control shRNAs were expressed in the pLKO puromycin-resistance vector (MISSION TRC shRNA Target Set; Sigma-Aldrich). We tested five different pLKO lentiviral vectors encoding PLC-β4-specific shRNA expression cassettes for their ability to knock down PLC-β4 expression in NIH3T3 cells; the pLKO-control (SHC002) served as a nontarget control shRNA contains nonhuman or mouse shRNA (5′-CAACAAGATGAAGAGCACCAA-3′).

To assess the efficacy of shRNAs, we transfected NIH3T3 cells with shRNA-expressing lentiviral vector constructs, and then determined the level of PLC-β4 expression in protein extracts by Western blot analysis using rabbit anti-PLC-β4 (1:200; Santa Cruz Biotechnology). To increase the levels of PLC-β4 expression in these selection experiments, we transfected NIH3T3 cells with the PLC-β4 expression plasmid, pFLAG-CMV2-PLC-β4. Expression levels were normalized to transfection efficiency, determined by cotransfection with a luciferase expression plasmid. Two of the PLC-β4-targeting shRNAs, shPLC-β4-1 (TRCN0000076919: 5′-GCCTCTTCAAAGTAGATGAAT-3′) and shPLC-β4-3 (TRCN0000076921: 5′-CCGTCTCCTAATGACCTCAAA-3′), reduced the level of PLC-β4 expression in cells cotransfected with lentiviral expression vectors (supplemental Fig. S1, available at www.jneurosci.org as supplemental material). shPLC-β4-1 was chosen for subsequent *in vivo* experiments.

Lentivirus-mediated knockdown of PLC-β4 in the medial septum in vivo. High-titer, concentrated lentiviral vectors (10^7 TU/μl) expressing shPLC-β4-1 or control shRNA were prepared and delivered into the medial septum of 10-week-old wild-type mice by stereotaxic injections (supplemental Fig. S2, available at www.jneurosci.org as supplemental material). Thirteen control shRNA mice and 16 mice injected with shPLC-β4-1 were used in this study. Four weeks after injections, mice were tested using the three anxiety tests, and then hippocampal EEGs were recorded as described below. After behavioral tests and EEG recording, mice were killed and evaluated immunohistochemically to assess the decrease of endogenous PLC-β4 expression in the medial septum. We observed a substantial reduction in PLC-β4 staining in shPLC-β4-1-infected neuronal cells of the medial septum, whereas neuronal cells from control shRNA mice showed normal PLC-β4 expression, confirming that lentiviruses expressing shPLC-β4 substantially reduce endogenous PLC-β4 expression in medial septal neurons.

Immunohistochemistry of the medial septum area. Tissues were processed and immunostained as previously described (Kim et al., 2008). Briefly, animals were perfused transcardially with PBS followed by 4%

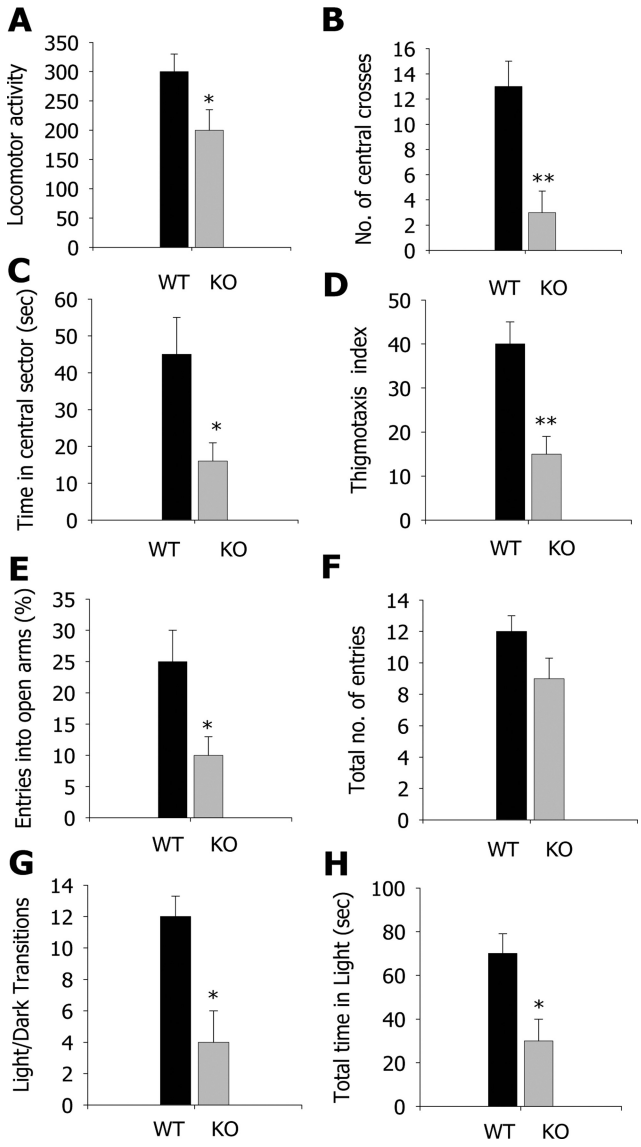

Figure 1. Increased anxiety behavior in PLC-$\beta4^{-/-}$ mice in open-field, elevated plus-maze, and light/dark transition tests. ***A***, Locomotor activity in the open field. ***B***, Number of central crosses in the open field. ***C***, Time in the central sector of the open field. ***D***, Thigmotaxis index: the lower the index, the higher the thigmotaxis (see Materials and Methods for detail). ***E***, Percentage entries into the open arms of the elevated plus-maze. ***F***, Total number of entries in the elevated plus-maze. ***G***, Light/dark transition number. ***H***, Total time in the light compartment. $^*p < 0.05$, $^{**}p < 0.01$, two-tailed *t* test; all data are presented as means ± SEM from 10 mice per genotypes.

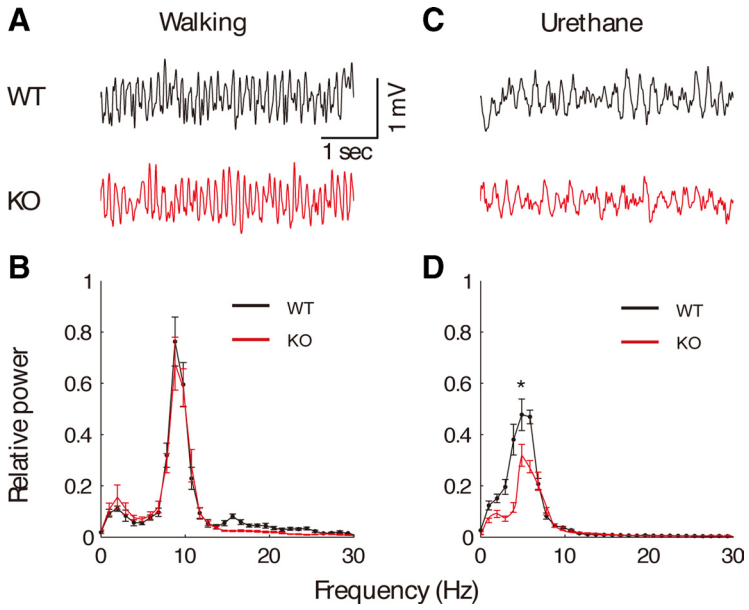

Figure 2. Intact noncholinergic theta rhythms and attenuated cholinergic theta rhythms in PLCβ-4 $^{-/-}$ mice. ***A***, Representative EEG waveforms during walking for wild-type mice (WT) and PLC-β4 $^{-/-}$ mice (KO). ***B***, Averaged power spectra of the EEG waveforms recorded during walking for wild-type mice ($n = 7$) and PLC-β4 $^{-/-}$ mice ($n = 7$). ***C***, Representative EEG waveforms during urethane anesthesia for wild-type mice (black trace) and PLC-β4 $^{-/-}$ mice (red trace). ***D***, Averaged power spectra of the EEG waveforms recorded during urethane anesthesia for wild-type mice ($n = 7$) and PLC-β4 $^{-/-}$ mice ($n = 7$). *$p < 0.05$, two-tailed *t* test; all data are presented as means ± SEM.

paraformaldehyde in 0.1 M phosphate buffer (PB), pH 7.4, under urethane anesthesia (1.5 g/kg, i.p.). The brains were removed and postfixed in the same fixative for 4 h. Brain tissues were cryoprotected by infiltration with 30% sucrose overnight. Thereafter, the entire medial septal area was frozen and sectioned with a cryostat into 30 μm sections and consecutive sections were placed in six-well plates containing PBS. Every sixth section in the series throughout the entire medial septal area from selected animals was used for the immunofluorescence study. The presence and absence of PLC-β4 expression in wild-type and PLC-β4 $^{-/-}$ mice, respectively, and morphological changes induced by shPLC-β4 in PLC-β4-positive neurons of the medial septal area were evaluated by double immunofluorescence staining for both mouse anti-neuronal nuclei (NeuN) IgG (1:100; Millipore Bioscience Research Reagents) and rabbit anti-PLC-β4 IgG (1:100; Millipore Bioscience Research Reagents). Brain tissues were incubated in the mixture of antisera overnight at room temperature. After washing three times with PBS (10 min each), sections were incubated in a mixture containing both Cy2-conjugated goat anti-mouse IgG (1:200; GE Healthcare) and Cy3-conjugated goat anti-rabbit IgG (1:200; GE Healthcare) for 1 h at room temperature. Sections were mounted in Vectashield mounting media with or without DAPI (4′,6′-diamidino-2-phenylindole) (Vector). Images were captured and analyzed using an Olympus DP50 digital camera and Viewfinder Life, version 1.0, software, or an Olympus FluoView FV1000 Confocal Microscope System. Figures were prepared using Adobe Photoshop 7.0. Manipulation of images was restricted to threshold and brightness adjustments applied to the entire image.

For quantification of PLC-β4 immunofluorescence in RNA interference (RNAi)-mediated PLC-β4 knockdown mice, we have performed the cell count in the medial septal area according to the previous description (Kim et al., 2008, 2009a,b). Briefly, PLC-β4 immunofluorescent images (10 sections/mice) were captured in the same region (500 × 500 μm). Images were sampled from at least five different points within each medial septum section. Thereafter, the number of PLC-β4-positive cells was actually counted within the sampled images. All immunoreactive cells were counted regardless the intensity of labeling. Cell counts were performed by two different investigators who were blind to the classification of tissues. The average percentage of PLC-β4 positive cells (C) in the medial septum of knock-down mice is estimated and shown as follows: $C = 100 \times (\sum Q_i/N_i)/K$, where Q_i is the actually counted numbers of PLC-β4-positive cells in the PLC-β4 viral vector-injected medial septum, N_i is the number of PLC-β4-positive cells in the control shRNA viral vector-injected animal groups, and K is the number of sampling.

All data obtained from the quantitative measurements were analyzed using one-way ANOVA to determine statistical significance. Bonferroni's test was used for *post hoc* comparisons. A value of $p < 0.05$ was considered statistically significant (Kim et al., 2008, 2009a,b).

Triple immunohistochemistry of the medial septal neurons. The specificity of PLC-β4 and glutamic acid decarboxylase (GAD) antibodies has been shown previously (Yamada et al., 2001; Nakamura et al., 2004). In the present study, we produced goat antibodies to PV and mGluR1a using the same fusion proteins as had been used for production of rabbit and guinea pig antibodies (Tanaka et al., 2000; Nakamura et al., 2004), and also to rat choline transporter 1 using C-terminal 50 aa sequence fused to glutathione *S*-transferase (Narushima et al., 2007). The procedures for fusion proteins, immunization, and affinity purification have been reported previously (Nakamura et al., 2004). The specificity of all these antibodies was checked by immunoblot detection of single protein bands and by selective immunohistochemical labeling of particular neuronal populations.

Animals were anesthetized by intraperitoneal injection with pentobarbital (100 mg/kg of body weight), fixed transcardially with 4% paraformaldehyde in 0.1 M sodium PB, pH 7.2, and subjected to preparation of coronal microslicer sections (50 μm in thickness; VT1000S, Leica). Before blocking with 10% normal donkey serum, sections were dipped successively in 30, 60, and 100% methanol or ethanol for 5 min each. Then they were incubated overnight in a mixture of guinea pig PLC-β4 antibody, rabbit antibody (GAD or mGluR1a), and goat antibody [mGluR1, PV, or choline transporter 1 (CHT1)], each being diluted to 1 μg/ml with PBS/0.1% Triton X-100 (TPBS). After washing in TPBS, sections were incubated for 2 h with a mixture of species-specific secondary antibodies (1:200 dilution) linked to Alexa 488 (Invitrogen), indocarbocyanine (Cy3), or indodicarbocyanine (Cy5) (Jackson ImmunoResearch). Images of single optical sections were taken with a confocal laser-scanning microscope (FV1000; Olympus). All images were obtained by restricting filter windows enough to eliminate each other and by adopting the sequential mode of laser scanning to minimize the bleedthrough.

Rescue experiments using rivastigmine. Rivastigmine (kindly provided by Novartis Pharma) was dissolved in saline. Animals were injected intraperitoneally with 0.5 mg/kg rivastigmine (total volume, 5 ml/kg) 60 min before the start of anxiety behavioral tests. This optimal dose of rivastigmine was chosen based on previously published microdialysis studies (Van Dam et al., 2005; Cerbai et al., 2007). Both PLC-β4 $^{+/+}$ (WT) and PLC-β4 $^{-/-}$ (KO) mice were randomly assigned to one of the following three treatment groups: (1) WT-sham (wild-type mice with intraperitoneal injection of saline; $n = 10$); (2) KO-sham (PLC-β4 $^{-/-}$ mice with intraperitoneal injection of saline; $n = 10$); and (3) KO-rivastigmine (PLC-β4 $^{-/-}$ mice with intraperitoneal injection of rivastigmine; $n = 10$).

Local field potential recordings in vivo. Hippocampal electroencephalogram (EEG) signals were recorded in mice (10–14 weeks of age) using published protocols (Shin and Talnov, 2001; Shin et al., 2005), with some modifications. Briefly, for electrode implantation, the animals were anesthetized with pentobarbital (50 ml/kg, i.p.) and held in a stereotaxic apparatus with bregma and lambda in the same horizontal plane. Hippocampal EEG recordings were performed using Teflon-coated tungsten electrodes (150 μm) implanted in the hippocampal fissure (from

bregma, 2.0 mm anteroposterior, 1.2 mm mediolateral, and 1.8 mm dorsoventral) with grounding over the cerebellum. The position of the electrodes was verified by light microscopy in Nissl-stained sections according to published protocols (Shin and Talnov, 2001; Shin et al., 2005). Field potential was amplified (1000×), bandpass-filtered (0.1–100 Hz), digitized with 16-bit resolution continuously at 1 kHz sampling, and recorded on a personal computer using Clampex 10 (MDS Analytical Technologies).

Analysis of hippocampal electrical activity data. EEG data were analyzed off-line according to published protocols (Shin and Talnov, 2001; Shin et al., 2005) using Clampfit 10 (MDS Analytical Technologies). Briefly, raw EEG data were collected in 4 s segments and fast-Fourier transformed off-line. The data were continuously monitored for movement artifacts, and the recording of each segment was manually verified by the experimenter, blinded to the genotype of the animals. All segments collected during mouse movements and those in which the amplitude of amplified EEG signals exceed a maximum of ±1.25 V were discarded to remove artifacts. To compare the EEG spectral characteristics of hippocampal electrical activities, we calculated EEG spectral power in 1 Hz bins using fast Fourier transformations (Hamming window) of each 4 s epoch. These analyses were performed on recordings from these intervals in 100 trials from each group. Powers in the 0–30 Hz range were averaged in groups across each behavioral state, and the mean values were plotted in 1 Hz bins. The averaging process for power spectrums used a normalization procedure that involved dividing by the combined SD of EEG raw data for the two comparison states (e.g., PLC-$\beta4^{-/-}$ mice and wild-type littermates) according to the previously published protocol (Shin et al., 2005). We used the peak power under different conditions for comparison purposes because the *in vivo* theta rhythm has a clear and sharp peak frequency that distinguished it from other *in vivo* EEG rhythms, such as delta- and gamma-band activities (Shin et al., 2005), and peak power provides more accurate information than total power in the theta frequency range.

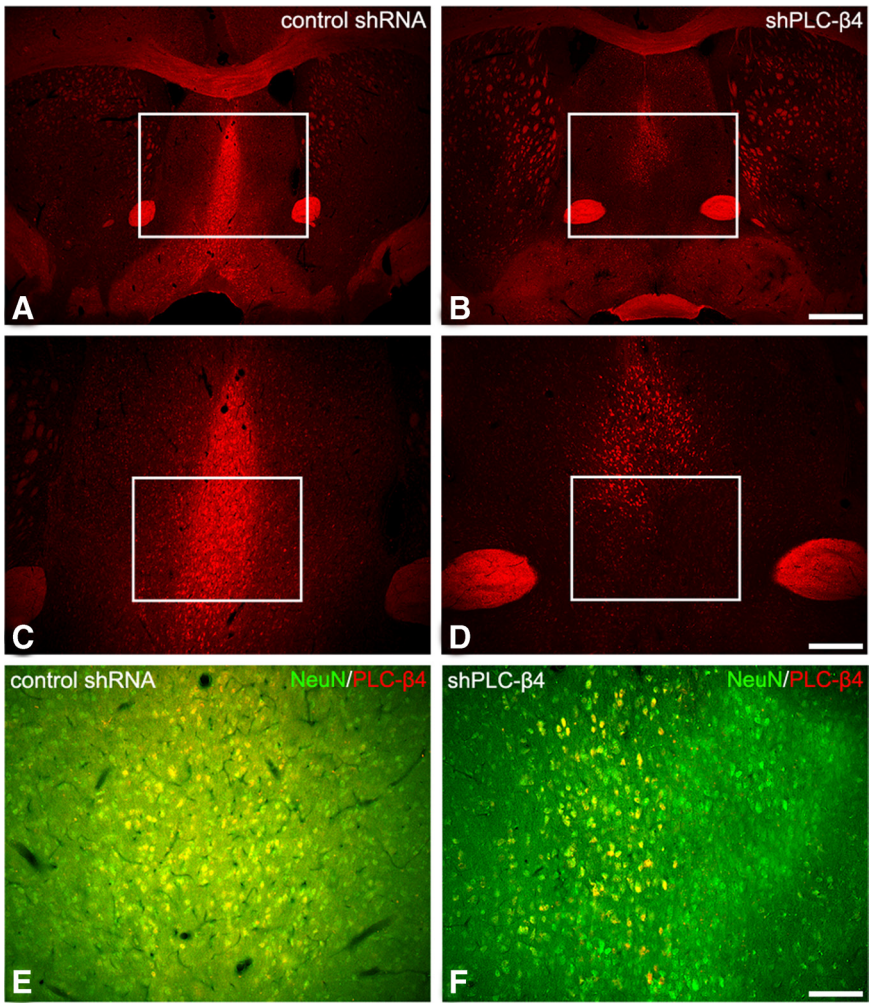

Figure 3. PLC-$\beta4$ expression in the medial septum of control shRNA mice and shPLC-$\beta4$ mice (***A–D***). Immunofluorescence staining for PLC-$\beta4$ in the medial septal area of shPLC-$\beta4$ mice is significantly downregulated (***B***, ***D***). A normal PLC-$\beta4$ expression pattern is observed in the control shRNA mice (***A***, ***C***). The rectangles in ***A*** and ***B*** indicate regions of ***C*** and ***D***. Scale bars: ***A***, ***B***, 280 μm; ***C***, ***D***, 100 μm. Coexpression of NeuN and PLC-$\beta4$ in control shRNA mice and shPLC-$\beta4$ mice (***E***, ***F***). Immunofluorescence staining for PLC-$\beta4$ in NeuN-positive neurons is markedly reduced in the medial septum of shPLC-$\beta4$ mice (***F***), whereas its expression in NeuN-positive neurons of control shRNA mice is generally unchanged (***E***). The rectangles in ***C*** and ***D*** indicate regions of ***E*** and ***F***. Scale bar: ***E***, ***F***, 50 μm.

Classification of cholinergic theta and noncholinergic theta rhythms associated with different behaviors. Cholinergic and noncholinergic theta rhythms associated with different behaviors were recorded according to published protocols (Shin and Talnov, 2001; Shin et al., 2005). Briefly, noncholinergic theta rhythms can be distinguished from cholinergic theta rhythms using muscarinic antagonists (e.g., atropine or scopolamine), which can abolish cholinergic theta rhythms when injected into the animal, but leave noncholinergic theta rhythms relatively unaffected (Bland, 1986). In addition, the use of different behaviors to induce theta rhythms can discriminate between noncholinergic theta rhythms and cholinergic theta rhythms. For example, cholinergic theta rhythms are generated normally during urethane anesthesia, alert immobility, and passive whole-body rotation (Bland, 1986; Shin et al., 2005; Shin, 2009). In contrast, noncholinergic theta rhythms are observed during locomotion activities, such as walking or running (Bland, 1986; Shin and Talnov, 2001). In addition, the two types of theta rhythms can usually be separated approximately (although not exclusively) into high- and low-frequency bands: 4–7 Hz for cholinergic type 2 theta rhythm, and 7–12 Hz for noncholinergic type 1 theta rhythm. However, several investigators have found that atropine-sensitive type 2 theta rhythms can have a frequency that is as high as the frequency limit of atropine-resistant type 1 theta rhythms under certain recording conditions (Bland and Oddie, 2002; Shin, 2009). Therefore, we did not use the high- and low-frequency theta bands to discriminate between cholinergic theta rhythm and noncholinergic theta rhythm.

In the present work, we have used urethane anesthesia, alert immobility and passive whole-body rotation to record cholinergic theta rhythms from wild-type and PLC-$\beta4^{-/-}$ mice, and from mice with medial septum-directed, shRNA-mediated PLC-$\beta4$ knockdown. Noncholinergic theta rhythms were recorded from mice walking in an open chamber or running on a wheel; the same mice were analyzed in both settings.

Anxiety behavioral tests. Three anxiety behavioral assays—open-field thigmotaxis, elevated plus-maze, and light/dark transition (see below)—were performed between 9:00 A.M. and 5:00 P.M. using adult (8- to 16-week-old) mice.

Thigmotaxis represents a mouse's natural tendency to stay near the perimeters of a novel environment (Treit and Fundytus, 1988). Open-field thigmotaxis was assessed by placing mice in the center of an open-field apparatus (40 × 40 × 40 cm) under dim lighting. During a 10 min observation period, locomotor activity, number of central crosses, and time spent in the central sector of the open field were recorded and

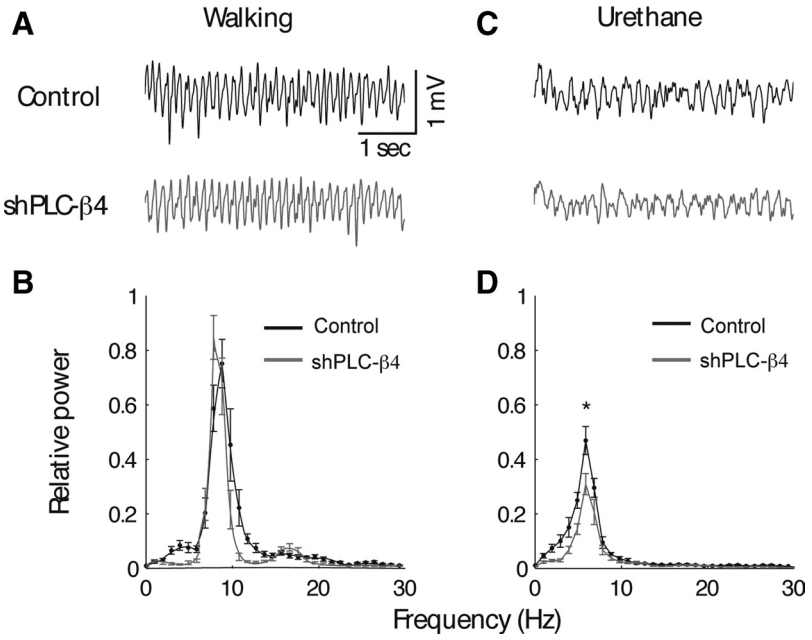

Figure 4. Medial septum-selective PLC-β4 knockdown replicates the theta rhythm heterogeneity phenotype of PLC-$\beta4^{-/-}$ mice. ***A***, Representative EEG waveforms during walking for wild-type mice injected with lentiviruses expressing control shRNA (control shRNA mice) and wild-type mice injected with lentivirus encoding shPLC-β4 (shPLC-β4 mice). ***B***, Averaged power spectra of the EEG waveforms recorded during walking for control shRNA mice ($n = 7$) and shPLC-β4 mice ($n = 7$). ***C***, Representative EEG waveforms during urethane anesthesia for control shRNA mice and shPLC-β4 mice. ***D***, Averaged power spectra of the EEG waveforms recorded during urethane anesthesia for control shRNA mice ($n = 7$) and shPLC-β4 mice ($n = 7$). *$p < 0.05$, two-tailed t test; all data are presented as means ± SEM.

analyzed using a PC-based video behavior analysis system (Noldus EthoVision 3.1; Noldus Information Technology). During analysis, the open field was divided into 36 small cubic areas using the software. Locomotor activity was defined as the number of crossing the small cubic areas during 10 min. The central sector of the open field with a distance of ~10 cm from the wall was defined as the central area. Thigmotaxis index was defined as a ratio of the number of entries into the central part of a testing arena to the locomotor activity, which then is multiplied by 1000. Thus, the lower the index, the higher the thigmotaxis. The thigmotaxis index was calculated for each mouse separately and used to calculate means and SEMs for a given experimental group (Treit and Fundytus, 1988; Sienkiewicz-Jarosz et al., 2000).

The apparatus used for the light/dark transition test consisted of a cage (25 × 40 × 20 cm) divided into two compartments by a black partition containing a small opening that allows the mouse to move from one compartment to the other. One compartment, comprising two-thirds of the surface area, was made of white plastic and was brightly illuminated; the adjoining smaller compartment was black and dark. Mice were placed in the dark compartment and allowed to move freely between the two chambers for 5 min. The number of transitions between the two compartments, time spent in each chamber, and latency to the first transition were recorded (Welch et al., 2007).

The elevated plus-maze consists of two open and two enclosed arms of the same size (45 × 5 cm) with walls 15 cm high. The arms, constructed of black acrylic, radiate from a central platform (5 × 5 cm) to form a plus sign. The entire apparatus was elevated to a height of 30 cm above floor level. Each mouse was placed in the central platform facing one of the open arms. The number of entries into the open and closed arms and the time spent on the open and closed arms were recorded during a 5 min test period (Gross et al., 2002; Santin et al., 2009).

Statistical analysis. Differences between groups were compared using Student's t test after confirming that data sets were normally distributed. Behavioral data for PLC-$\beta4^{-/-}$ mice, wild-type littermates, and rivastigmine-treated PLC-$\beta4^{-/-}$ mice were analyzed by ANOVA followed by Tukey's *post hoc* test to determine differences among groups.

Results

Increased anxiety behaviors in PLC-$\beta4^{-/-}$ mice

We tested PLC-$\beta4^{-/-}$ mice in three anxiety behavioral assays: open field, elevated plus-maze, and light/dark box. In the open-field assay, PLC-$\beta4^{-/-}$ mice showed reduced locomotion in the open field (quantified as described in Materials and Methods) compared with wild-type mice (Fig. 1*A*) ($p = 0.022$, Student's t test). The PLC-$\beta4^{-/-}$ mice crossed the aversive center of the open field less frequently than did wild-type mice (Fig. 1*B*) ($p = 0.001$, Student's t test) and spent less time in the central sector of the open field (Fig. 1*C*) ($p = 0.015$, Student's t test). Thus, thigmotaxis, a mouse's natural tendency to stay near the perimeters of a novel environment (Treit and Fundytus, 1988), was enhanced in PLC-$\beta4^{-/-}$ mice compared with wild-type littermates (Fig. 1*D*) ($p = 0.002$, Student's t test). In the elevated plus-maze, PLC-$\beta4^{-/-}$ mice made fewer entries into the aversive open arms compared with wild-type mice (Fig. 1*E*) ($p = 0.014$, Student's t test). The total number of entries (closed plus open arms) did not differ between the two groups (Fig. 1*F*) ($p = 0.4$, Student's t test). Similarly, in the light/dark box test, PLC-$\beta4^{-/-}$ mice made fewer transitions from the dark to the light compartment than did wild-type mice (Fig. 1*G*) ($p = 0.01$, Student's t test). Consistent with this, the time spent in the light chamber was significantly shorter for PLC-$\beta4^{-/-}$ mice than for wild-type mice (Fig. 1*H*) ($p = 0.019$, Student's t test). Together, these results demonstrate a higher level of anxiety in PLC-$\beta4^{-/-}$ mice compared with wild-type mice.

Profile of theta rhythms in PLC-$\beta4^{-/-}$ mice

To determine whether the theta rhythm profile is changed in PLC-$\beta4^{-/-}$ mice and, if so, whether the difference is attributable to cholinergic or noncholinergic theta rhythms, we examined hippocampal EEG in PLC-$\beta4^{-/-}$ and wild-type littermates using previously established protocols and criteria (Shin et al., 2005), as described in Materials and Methods.

Noncholinergic theta rhythm

Locomotion, including walking and running, is accompanied by noncholinergic theta rhythms. To investigate theta rhythms generated during locomotion in PLC-$\beta4^{-/-}$ mice, we recorded hippocampal electrical activities while mice were walking. Figure 2*A* shows that theta rhythms recorded during this locomotion were similar in both PLC-$\beta4^{-/-}$ mice and wild-type littermates. The maximum EEG power in the theta band of 4–12 Hz also did not significantly differ between PLC-$\beta4^{-/-}$ mice and wild-type littermates ($p > 0.1$, Student's t test) (Fig. 2*B*).

Cholinergic theta rhythm

As a first step to characterizing cholinergic theta rhythms *in vivo* in the mutant mice, we performed spontaneous hippocampal EEG recordings of mice anesthetized with urethane (1 g/kg, i.p.). This procedure is known to induce isolated cholinergic theta

rhythms (Bland, 1986). In both PLC-$\beta4^{-/-}$ mice and wild-type littermates, urethane induced intermittent theta rhythms that were clearly evident in hippocampal fissure recordings collected in undisturbed mice (Fig. 2*C*). However, a power spectral analysis showed that theta power was significantly reduced in PLC-$\beta4^{-/-}$ mice compared with wild-type littermates (Fig. 2*D*) ($p < 0.05$, Student's t test). In addition to spontaneous urethane anesthesia condition, alert immobility as well as passive-whole-body rotation have been previously shown to induce isolated cholinergic theta rhythm (Shin et al., 2005; Shin, 2009). Consistent with the results from the spontaneous urethane anesthesia condition, we found that cholinergic theta rhythms generated during alert immobility or passive-whole-body rotation were smaller in PLC-$\beta4^{-/-}$ mice than in wild-type littermates (supplemental Fig. S3, available at www.jneurosci.org as supplemental material).

Short hairpin RNA-mediated PLC-β4 gene silencing in the medial septum

Preexisting evidence demonstrating a role for the medial septum in controlling theta rhythms (Bland, 1986) and predominant PLC-$\beta4$ expression in the medial septum area (supplemental Fig. S4, available at www.jneurosci.org as supplemental material) led us to hypothesize that the loss of PLC-$\beta4$ in the medial septum might be responsible both for the increased anxiety behavior and attenuated cholinergic theta rhythm observed in PLC-$\beta4^{-/-}$ mice. To further verify the causal relationship between PLC-$\beta4$ ablation in the medial septum and these two phenotypic properties, we used shRNA-mediated gene silencing to specifically knockdown PLC-$\beta4$ gene expression (see Materials and Methods) (supplemental Fig. S1, available at www.jneurosci.org as supplemental material). Lentiviral vectors expressing PLC-$\beta4$-targeting shRNA (shPLC-$\beta4$) or control shRNA were delivered to the medial septum of 10-week-old wild-type mice (supplemental Fig. S2, available at www.jneurosci.org as supplemental material) (see Materials and Methods). In postmortem examinations of brains at the end of the study, we observed a substantial reduction in PLC-$\beta4$ staining in neuronal cells of the medial septum of the mice injected with shPLC-$\beta4$ lentiviruses (shPLC-$\beta4$ mice) compared with that in mice injected with the control lentiviruses (control shRNA mice) (Fig. 3). To quantify the amount of gene silencing of the medial septum, we analyzed the percentage of PLC-$\beta4$-positive neurons in the medial septum after shPLC-$\beta4$ lentiviral vector injection compared with the control shRNA-injected mice. We found that, after shPLC-$\beta4$ lentiviral vector injection, the average percentage of PLC-$\beta4$-positive neurons was significantly reduced down to 39.1 ± 10.6% compared with control in the medial septum ($p < 0.05$) (supplemental Fig. S5, available at www.jneurosci.org as supplemental material).

Next, we investigated whether lentivirus-mediated selective knockdown of PLC-$\beta4$ expression in medial septal neurons attenuated cholinergic theta rhythms and/or increased anxiety levels, thus replicating the phenotype of PLC-$\beta4^{-/-}$ mice. Cholinergic theta rhythms recorded during urethane anesthesia were attenuated in shPLC-$\beta4$ mice compared with control shRNA mice (Fig. 4*C*,*D*), whereas noncholinergic theta rhythms observed during locomotion (i.e., walking) remained intact (Fig. 4*A*,*B*). Next, we tested shPLC-$\beta4$ mice and control shRNA mice in the three anxiety behavioral assays. In the open-field assay, shPLC-$\beta4$ mice showed no significant difference in the total amount of locomotion activities in the open field compared with control shRNA mice (Fig. 5*A*) ($p = 0.897$, Student's t test). However, shPLC-$\beta4$ mice crossed the aversive center of the open field less often than did control shRNA mice (Fig. 5*B*) ($p = 0.02$, Student's t test) and spent less time in the central sector of the open field (Fig. 5*C*) ($p = 0.041$, Student's t test). Thus, thigmotaxis, a mouse's natural tendency to stay near the perimeters of a novel environment, was enhanced in shPLC-$\beta4$ mice than in control shRNA mice (Fig. 5*D*) ($p = 0.006$, Student's t test). In the elevated plus-maze test, shPLC-$\beta4$ mice made fewer entries into the aversive open arms compared with control shRNA mice (Fig. 5*E*) ($p < 0.001$, Student's t test); the total number of entries (closed plus open arms) did not differ between the two groups (Fig. 5*F*) ($p = 0.128$, Student's t test). Similarly, in the light/dark box test, shPLC-$\beta4$ mice made fewer transitions from the dark to the light compartment compared with shRNA mice (Fig. 5*G*) ($p = 0.01$, Student's t test). Consistent with this observation, shPLC-$\beta4$ mice stayed a significantly shorter time in the light chamber than did control shRNA mice (Fig. 5*H*) ($p = 0.047$, Student's t test). These results confirm that the attenuated cholinergic theta rhythm and increased anxiety behavior phenotypes of the PLC-$\beta4^{-/-}$ mice were primarily attributable to the elimination of PLC-$\beta4$ proteins from the medial septum.

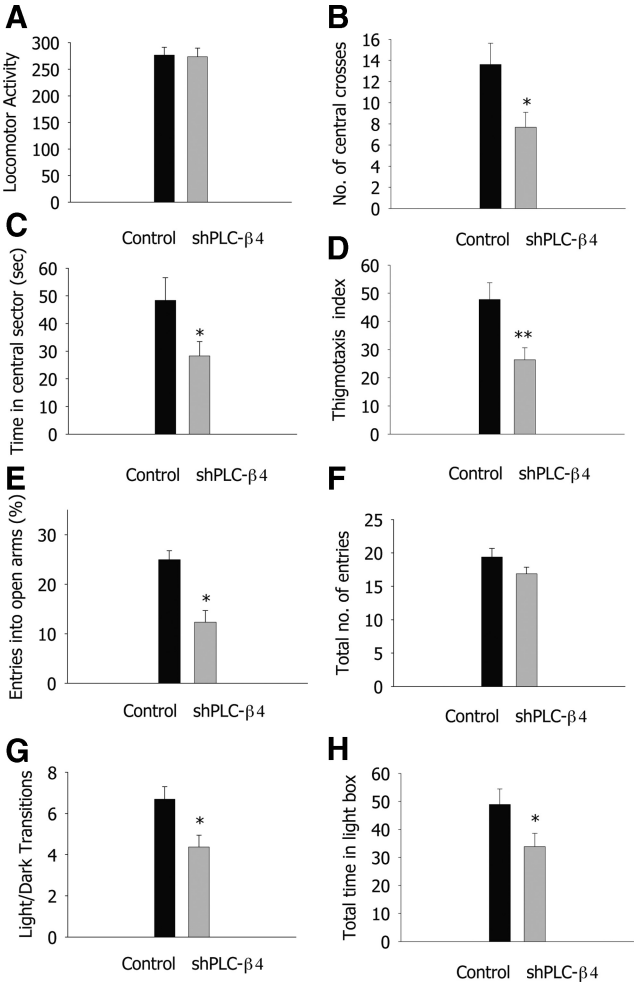

Figure 5. Medial septum-selective PLC-$\beta4$ knockdown replicates the anxiety behavior phenotype of PLC-$\beta4^{-/-}$ mice. ***A***, Locomotor activity in the open field. ***B***, Number of central crosses in the open field. ***C***, Time in the central sector of the open field. ***D***, Thigmotaxis index. ***E***, Percentage entries into the open arms of the elevated plus-maze. ***F***, Total number of entries in the elevated plus-maze. ***G***, Light/dark transition number. ***H***, Total time in the light compartment. $^*p < 0.05$, $^{**}p < 0.01$, $^{***}p < 0.001$, two-tailed t test; $n = 13$ for control shRNA mice and $n = 16$ for shPLC-$\beta4$ mice; all data are presented as means ± SEM from 10 mice per genotypes.

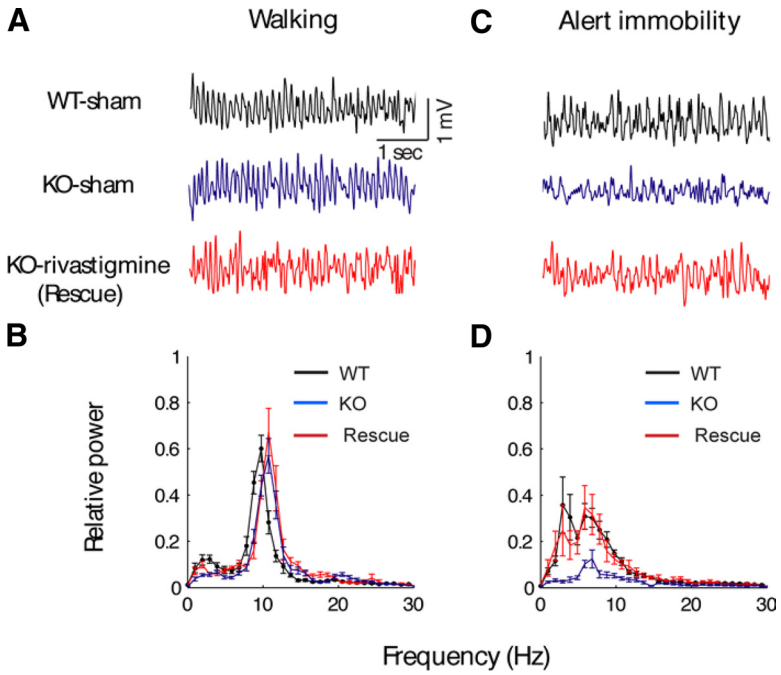

Figure 6. Rivastigmine rescues impaired cholinergic theta rhythms in PLC-$\beta4^{-/-}$ mice. ***A***, Representative EEG waveforms during walking for wild-type mice with intraperitoneal injection of saline (WT-sham), PLC-$\beta4^{-/-}$ mice with intraperitoneal injection of saline (KO-sham), and PLC-$\beta4^{-/-}$ mice with intraperitoneal injection of rivastigmine (KO-rivastigmine). ***B***, Averaged power spectra of the EEG waveforms recorded during walking for WT-sham ($n = 10$), KO-sham ($n = 10$), and KO-rivastigmine ($n = 10$). ***C***, Representative EEG waveforms during alert immobility for WT-sham (black trace), KO-sham (blue trace), and KO-rivastigmine (red trace). ***D***, Averaged power spectra of the EEG waveforms recorded during alert immobility for WT-sham ($n = 10$), KO-sham ($n = 10$), and KO-rivastigmine ($n = 10$). All data are presented as means ± SEM.

Rescue of the PLC-$\beta4^{-/-}$ cholinergic theta rhythm and anxiety phenotypes by rivastigmine

In both PLC-$\beta4^{-/-}$ mice and shPLC-$\beta4$ mice, we found that the attenuated cholinergic theta rhythms are associated with increased anxiety phenotype. To further confirm the interrelationship between cholinergic theta rhythms and anxiety behavior, we designed an experiment to determine whether increasing cholinergic transmission in PLC-$\beta4^{-/-}$ mice could rescue the attenuated amplitude of cholinergic theta rhythms, and thereby normalize the attendant anxiety behavior. To this end, we administered the cholinergic-enhancing drug, rivastigmine, an acetylcholinesterase inhibitor known to increase the cholinergic transmission in the septohippocampal pathway (Wu et al., 2003b; Van Dam et al., 2005; Cerbai et al., 2007).

Restoration of normal cholinergic theta rhythms in PLC-$\beta4^{-/-}$ mice by rivastigmine

To investigate whether rivastigmine treatment could rescue attenuated cholinergic theta rhythms in PLC-$\beta4^{-/-}$ mice, we recorded EEGs from three groups of mice: (1) PLC-$\beta4^{-/-}$ mice injected with rivastigmine, (2) PLC-$\beta4^{-/-}$ mice injected with saline, and (3) wild-type littermates injected with saline, after placing them in a new environment. Human theta rhythm associated with anxiety has traditionally been recorded in patients performing mental activities without movement in a novel environment (Mizuki et al., 1989; Suetsugi et al., 2000). To recapitulate this behavioral condition as closely as possible, we chose the novel-environment model, which induces alert-immobility states and evokes anxiety, among several conditions known to generate cholinergic theta rhythm in mice (see Materials and Methods).

Both noncholinergic and cholinergic theta rhythms appeared when mice were placed in a new environment. The amplitude of theta rhythms recorded during locomotion (i.e., walking) in the new open field was not significantly different among the three groups (Fig. 6*A*,*B*). However, in saline-injected PLC-$\beta4^{-/-}$ mice, cholinergic theta rhythms recorded during alert-immobility state in the new open field were attenuated compared with saline-injected wild-type littermates (Fig. 6*C*,*D*). Importantly, in PLC-$\beta4^{-/-}$ mice treated with rivastigmine (0.5 mg/kg, i.p.), the amplitude of the cholinergic theta rhythm was restored to a level similar to that of wild-type littermates injected with saline (Fig. 6*C*,*D*). These results suggest that increasing cholinergic transmission in the septohippocampal pathway rescued the attenuated cholinergic theta rhythms in PLC-$\beta4^{-/-}$ mice.

Attenuation of abnormal anxiety behaviors in PLC-$\beta4^{-/-}$ mice by rivastigmine

Next, we tested whether rivastigmine administration could also rescue the increased anxiety phenotype of PLC-$\beta4^{-/-}$ mice. We injected rivastigmine (0.5 mg/kg, i.p.) into PLC-$\beta4^{-/-}$ mice and, 60 min after injection, tested the rivastigmine-treated group in the three anxiety behavioral assays. In each of the three anxiety tests, the rivastigmine-treated group showed normal levels of anxiety, demonstrating a reversal of the increased anxiety phenotype of the PLC-$\beta4^{-/-}$ mice (Fig. 7). In the open-field test, PLC-$\beta4^{-/-}$ mice injected with saline showed an overall decrease in locomotion (Fig. 7*A*) (ANOVA, $F_{(2,25)} = 4.26$, $p = 0.022$) and moved less in the aversive center of the open field than did saline-injected wild-type littermates (Fig. 7*B*) (ANOVA, $F_{(2,25)} = 7.60$, $p = 0.002$). However, PLC-$\beta4^{-/-}$ mice injected with rivastigmine showed wild-type levels of locomotion in the center of the open field as well as wild-type levels of total locomotion activities (Fig. 7*A*,*B*). Rivastigmine administration also restored the amount of time spent in the central sector of the open field to levels comparable with those in wild-type mice injected with saline (Fig. 7*C*). Finally, rivastigmine also rescued thigmotaxis index to the same levels as those in wild-type mice injected with saline (Fig. 7*D*). In the elevated plus-maze, PLC-$\beta4^{-/-}$ mice injected with saline made fewer entries into the aversive open arms, whereas the behavior of the rivastigmine-treated group was indistinguishable from that of wild-type littermates injected with saline (Fig. 7*E*). Total entries into the closed and open arms did not differ among the three groups (Fig. 7*F*) (ANOVA, $F_{(2,25)} = 0.41$, $p = 0.48$). Similarly, in the light/dark box test, PLC-$\beta4^{-/-}$ mice injected with saline made fewer transitions between light and dark boxes (Fig. 7*G*) (ANOVA, $F_{(2,25)} = 7.90$, $p = 0.021$) and spent significantly less time in the light chamber (Fig. 7*H*) (ANOVA, $F_{(2,25)} = 5.2$, $p = 0.029$) than did saline-injected wild-type littermates. In both cases, the behavior of rivastigmine-treated PLC-$\beta4^{-/-}$ mice was indistinguishable from that of wild-type littermates injected with saline. Together, these data show that rivastigmine treatment is sufficient to restore both normal cholinergic theta rhythms and normal anxiety behavior in PLC-

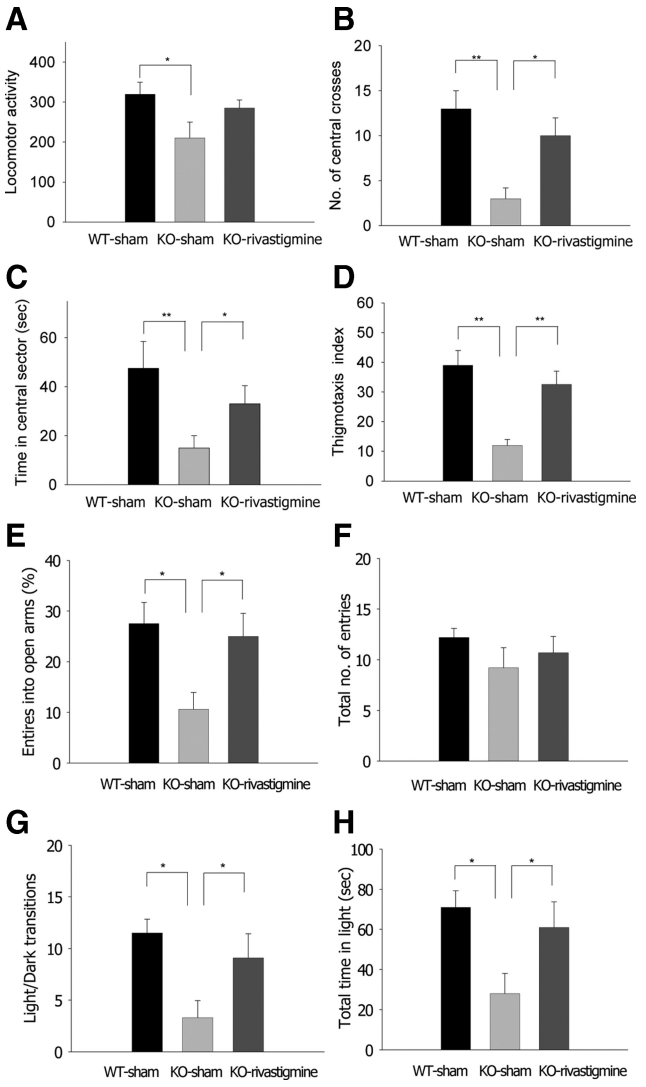

Figure 7. Rivastigmine rescues increased anxiety behavior of PLC-$\beta4^{-/-}$ mice. ***A***, Locomotor activity in the open field. ***B***, Number of central crosses in the open field. ***C***, Time in the central sector of the open field. ***D***, Thigmotaxis index. ***E***, Percentage entries into the open arms of the elevated plus-maze. ***F***, Total number of entries in the elevated plus-maze. ***G***, Light/dark transition number. ***H***, Total time in the light compartment. $*p < 0.05$, $**p < 0.01$, ANOVA; all data are presented as means ± SEM from 10 mice per group.

$\beta4^{-/-}$ mice, and suggest that cholinergic theta rhythms play a critical role in suppressing anxiety.

Triple immunohistochemistry of the medial septum

It is known that cholinergic and GABAergic neurons are the two major groups of neurons in the medial septum (Bland, 1986; Buzsáki, 2002). Attenuated cholinergic theta rhythm but intact noncholinergic theta rhythm shown in PLC-$\beta4^{-/-}$ mice suggests that cholinergic and/or GABAergic neurons in the medial septum may be affected in these mutant mice. Thus, it is essential to know the expression pattern of PLC-$\beta4$ in the medial septum to understand the underlying mechanism of attenuated cholinergic theta rhythm found in the PLC-$\beta4^{-/-}$ mice. Therefore, we performed immunohistochemistry of the medial septal neurons, using a series of antibodies, such as ones against PLC-$\beta4$, GAD, mGluR1a, PV, or CHT1 proteins (see Materials and Methods). In the medial septum, PLC-$\beta4$ was detected in a particulate pattern of immunostaining inside neuronal perikarya and thick processes (presumed dendrites), as reported in other brain regions (Nakamura et al., 2004). PLC-$\beta4$ was expressed in almost all of GAD-positive neurons (Fig. 8*A–C*, neurons 1 through 8; *E–G*, neurons 1 through 5). By counting the number of neuronal profiles having the nucleus, 91 of 99 PLC-$\beta4$-expressing neurons were found to be GAD-positive. In many of these neurons, mGluR1a was detected as surface labeling of cell bodies or as low heterogeneous labeling inside the perikarya; the latter labeling was sometimes difficult to be discriminated from background labeling. When we adopted the former labeling for the criteria of mGluR1a-positive neurons, mGluR1a was detected in nearly one-half (25 of 51) of PLC-$\beta4$-expressing GABAergic neurons (Fig. 8*D*, neurons 2, 3, 5, and 8; *L*, neuron 1). These results agree with the previous reports which show that mGluR1a is coupled to PLC-$\beta4$ (Kim et al., 1997; Nakamura et al., 2004). In addition, one-third (19 of 53) of PLC-$\beta4$-expressing GABAergic neurons were labeled for PV either intensely (Fig. 8*H*, neuron 5; *K*, neuron 3) or weakly (Fig. 8*H*, neurons 3 and 4; *K*, neuron 2). Intense perikaryal labeling is the level higher than adjacent neuropil labeling, and weak labeling is that lower than adjacent neuropil labeling. When examined simultaneously (Fig. 8*I–L*), mGluR1 (Fig. 8*L*, neuron 1) and PV (Fig. 8*K*, neurons 2 and 3) were generally detected in distinct populations, but there are some neurons labeled (data not shown) or unlabeled (Fig. 8*I–L*, neuron 4) for the two.

Intense labeling for PLC-$\beta4$, whose intensity in perikarya was apparently higher than that in adjacent neuropils, was occasionally detected in GAD-negative neuronal profiles (Fig. 8*A–D*, yellow arrows). By counting the number of neuronal profiles having the nucleus, 3 of 83 PLC-$\beta4$-expressing neurons were labeled for CHT1, a marker for cholinergic neurons (Fig. 8*M–P*). These cholinergic neurons had relatively large perikarya and exhibited intense labeling for PLC-$\beta4$. We also encountered a small number of PLC-$\beta4$-expressing neurons that were negative for GAD and CHT1.

These results indicate that GABAergic neurons are the major PLC-$\beta4$-expressing neurons in the medial septum, and cholinergic neurons, although a few in number, highly express PLC-$\beta4$.

Discussion

This report shows that the PLC-$\beta4^{-/-}$ mouse exhibited an attenuated cholinergic theta rhythm and an accompanying increase in the anxiety level. Furthermore, we demonstrated a possible causal relationship between cholinergic theta rhythm and the anxiety level using a combination of tissue-specific gene-knockdown and pharmacological rescue strategies. This is the first report to reveal that attenuated cholinergic theta rhythm is critically related to increased anxiety.

Anomalies of medial septal nuclei within the basal forebrain are involved in abnormal information processing at cortical circuits and are responsible for consequent brain dysfunctions, as shown in Alzheimer's disease (Kesner et al., 1989; Colom, 2006), Down's syndrome (Chen et al., 2009), Lewy body disease (Fujishiro et al., 2006), and Parkinson's disease (Dodel et al., 2008). Interestingly, anxiety is common among patients with diverse forms of dementia and other neurological disorders (Porter et al., 2003). By selectively knocking down PLC-$\beta4$ expression in medial septal neurons using lentiviral-mediated RNAi, we demonstrated that the medial septum is critically involved in both attenuated cholinergic theta rhythm and increased anxiety observed in the PLC-$\beta4^{-/-}$ mice (Figs. 4, 5). The amplitude of cholinergically mediated hippocampal theta rhythms depends on the coactivation of cholinergic and GABAergic inputs from the medial septum to the hippocampus (Smythe et al., 1992). Cho-

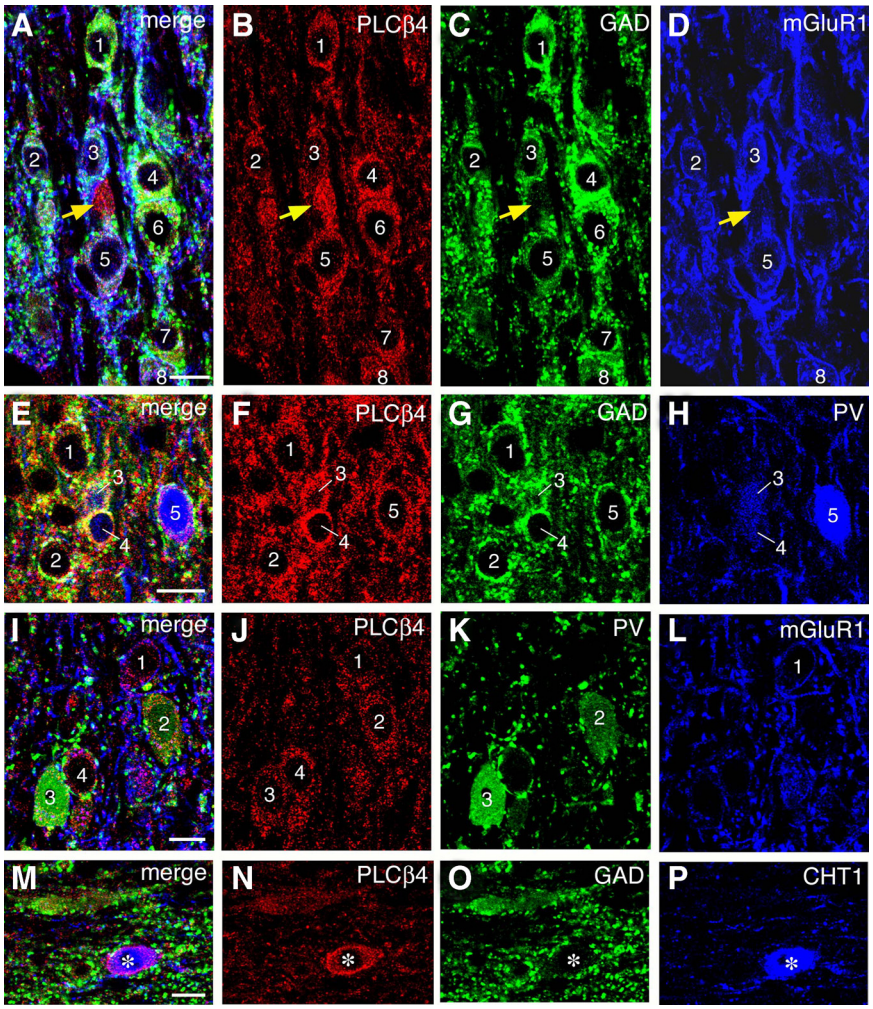

Figure 8. Triple immunofluorescence showing that PLC-β4 is detected in GABAergic neurons expressing mGluR1a and PV and in cholinergic neurons expressing CHT1. Triple labeling for PLC-β4, GAD, and mGluR1 (***A–D***), PLC-β4, GAD, and PV (***E–H***), PLC-β4, PV, and mGluR1 (***I–L***), and PLC-β4, GAD, and CHT1 (***M–P***). Labeled neurons are indicated by numerals. Note infrequent and intense PLC-β4 labeling in GAD-negative neuronal elements (***A–D***, yellow arrows), which are likely to represent cholinergic neurons expressing CHT1 (***M–P***). Scale bars, 10 μm.

linergic projections provide the afferent excitatory drive, and GABAergic projections act to reduce the overall level of inhibition in the hippocampus by inhibiting inhibitory hippocampal GABAergic interneurons (i.e., a disinhibition mechanism) (Smythe et al., 1992). We found by immunohistochemistry that PLC-β4 is detected in GABAergic neurons expressing parvalbumin and in a few cholinergic neurons expressing choline transporter 1 in the medial septum (Fig. 8). The mGluR1a has been shown to lie upstream of PLC-β4 in the medial septum (Nakamura et al., 2004), and mGluR1a antagonists have been shown to decrease the firing rate of both septohippocampal cholinergic and GABAergic neurons in the medial septum (Wu et al., 2003a, 2004). Interestingly, acetycholinesterase inhibitors have been shown to not only increase the acetylcholine concentration in the hippocampus (Van Dam et al., 2005; Cerbai et al., 2007) but also to enhance GABAergic neuronal firing rate in the medial septum (Wu et al., 2003b). Therefore, administration of an acetylcholine esterase inhibitor to PLC-$\beta4^{-/-}$ mice might be expected to recover attenuated cholinergic theta rhythms in the mutant. We confirmed this prediction using the acetylcholinesterase inhibitor, rivastigmine, which successfully rescued both the attenuated cholinergic theta rhythm and increased anxiety phenotypes of PLC-$\beta4^{-/-}$ mice (Figs. 6, 7). Therefore, together with previously published reports suggesting that the mGluR1a–PLC-β4 signaling pathway is involved in modulating neuronal excitability such as firing rate (Shin et al., 1999; Miyata et al., 2003; Park et al., 2003, Cheong et al., 2008), our present results suggest that abolition of PLC-β4 in the medial septal GABAergic and cholinergic neurons may reduce cholinergic theta amplitude via two mechanisms: (1) the decreased GABAergic input to the hippocampus reduces the overall level of disinhibition in the hippocampus and, thus, contributes to the attenuated cholinergic theta rhythm; and (2) the attenuated firing activity of medial septal cholinergic neurons reduces acetylcholine in the hippocampus and the medial septum, which contributes to the attenuated cholinergic theta rhythm. In summary, (1) ascending excitatory drive activated GABAergic and cholinergic neurons via mGluR1a acting through PLC-β4, and (2) glutamatergic and cholinergic excitation converge on the medial septum GABAergic neuron population primarily responsible for generating the rhythmic disinhibition of pyramidal cells in the hippocampus.

The importance of the neurotransmitter, 5-HT, in the pathophysiology of anxiety is well known (Toth, 2003; Gordon and Hen, 2004), and a key role for postsynaptic $5HT_{1A}$ receptors in anxiety has been suggested based on studies using $5HT_{1A}$ receptor knock-out ($5HT_{1A}^{-/-}$) mice (Parks et al., 1998; Ramboz et al., 1998). A receptor binding study using positron emission tomography confirmed that postsynaptic $5HT_{1A}$ receptor levels were reduced in untreated anxiety patients compared with controls (Lanzenberger et al., 2007). Interestingly, a recent study demonstrated a positive correlation between theta rhythms generated during locomotion and the anxiety level in $5HT_{1A}^{-/-}$ mice (Gordon et al., 2005). On the other hand, it has been well established that both serotonergic and GABAergic anxiolytic drugs reduce the frequency of hippocampal theta rhythms elicited by brainstem electrical stimulations (McNaughton et al., 2007), whereas a cholinergic drug, acetylcholinesterase inhibitor, did not change the theta frequency under the same conditions (Kinney et al., 1999). Together with these previous observations, our present results suggest that the theta rhythm heterogeneity is associated with different biochemical and behavioral conditions, and may provide useful insights into designing rational drug treatment for heterogenous anxiety disorders.

Mild cognitive impairment (MCI) is an etiologically heterogeneous condition characterized by cognitive changes that are insufficient to represent dementia and do not impair daily living activities (Mariani et al., 2007). Ongoing research is focused on identifying those individuals with MCI who are most likely to convert to Alzheimer's disease (AD) (Levey et al., 2006). Several lines of evidence suggest that MCI patients with both memory

deficits and neuropsychiatric manifestations, such as anxiety, are more prone to develop AD than patients without these features (Apostolova and Cummings, 2008). Our demonstration here that attenuated cholinergic theta rhythms are accompanied by increased anxiety, as well as preexisting evidence for a critical role for cholinergic theta rhythms in memory formation (Shin, 2002; Shin et al., 2005), suggest that measuring the cholinergic theta rhythm profile may be a potentially useful tool for identifying which MCI patients are more prone to convert to AD.

References

Apostolova LG, Cummings JL (2008) Neuropsychiatric manifestations in mild cognitive impairment: a systematic review of the literature. Dement Geriatr Cogn Disord 25:115–126.

Bland BH (1986) The physiology and pharmacology of hippocampal formation theta rhythms. Prog Neurobiol 26:1–54.

Bland BH, Oddie SD (2002) Theta band oscillation and synchrony in the hippocampal formation and associated structures: the case for its role in sensorimotor integration. Behav Brain Res 127:119–136.

Buzsáki G (2002) Theta oscillations in the hippocampus. Neuron 33:325–340.

Cerbai F, Giovannini MG, Melani C, Enz A, Pepeu G (2007) N1phenethylnorcymserine, a selective butyrylcholinesterase inhibitor, increases acetylcholine release in rat cerebral cortex: a comparison with donepezil and rivastigmine. Eur J Pharmacol 572:142–150.

Chen Y, Dyakin VV, Branch CA, Ardekani B, Yang D, Guilfoyle DN, Peterson J, Peterhoff C, Ginsberg SD, Cataldo AM, Nixon RA (2009) In vivo MRI identifies cholinergic circuitry deficits in a Down syndrome model. Neurobiol Aging 30:1453–1465.

Cheong E, Lee S, Choi BJ, Sun M, Lee CJ, Shin HS (2008) Tuning thalamic firing modes via simultaneous modulation of T- and L-type Ca^{2+} channels controls pain sensory gating in the thalamus. J Neurosci 28:13331–13340.

Colom LV (2006) Septal networks: relevance to theta rhythm, epilepsy and Alzheimer's disease. J Neurochem 96:609–623.

Dodel R, Csoti I, Ebersbach G, Fuchs G, Hahne M, Kuhn W, Oechsner M, Jost W, Reichmann H, Schulz JB (2008) Lewy body dementia and Parkinson's disease with dementia. J Neurol 255:S39–S47.

Fujishiro H, Umegaki H, Isojima D, Akatsu H, Iguchi A, Kosaka K (2006) Depletion of cholinergic neurons in the nucleus of the medial septum and the vertical limb of the diagonal band in dementia with Lewy bodies. Acta Neuropathol 111:109–114.

Gordon JA, Hen R (2004) The serotonergic system and anxiety. Neuromolecular Med 5:27–40.

Gordon JA, Lacefield CO, Kentros CG, Hen R (2005) State-dependent alterations in hippocampal oscillations in serotonin 1A receptor-deficient mice. J Neurosci 25:6509–6519.

Gray JA, McNaughton N (2000) The neuropsychology of anxiety, Ed 2. New York: Oxford UP.

Gross C, Zhuang X, Stark K, Ramboz S, Oosting R, Kirby L, Santarelli L, Beck S, Hen R (2002) Serotonin1A receptor acts during development to establish normal anxiety-like behaviour in the adult. Nature 416:396–400.

Hwang JI, Shin KJ, Oh YS, Choi JW, Lee ZW, Kim D, Ha KS, Shin HS, Ryu SH, Suh PG (2005) Phospholipase C-beta3 mediates the thrombin-induced Ca^{2+} response in glial cells. Mol Cells 19:375–381.

Kesner RP, Adelstein TB, Crutcher KA (1989) Equivalent spatial location memory deficits in rats with medial septum or hippocampal formation lesions and patients with dementia of the Alzheimer's type. Brain Cogn 9:289–300.

Kim D, Jun KS, Lee SB, Kang NG, Min DS, Kim YH, Ryu SH, Suh PG, Shin HS (1997) Phospholipase C isozymes selectively couple to specific neurotransmitter receptors. Nature 389:290–293.

Kim DS, Kim JE, Kwak SE, Choi KC, Kim DW, Kwon OS, Choi SY, Kang TC (2008) Spatiotemporal characteristics of astroglial death in the rat hippocampo-entorhinal complex following pilocarpine-induced status epilepticus. J Comp Neurol 511:581–598.

Kim JE, Kwak SE, Kang TC (2009a) Upregulated TWIK-related acid-sensitive K^+ channel-2 in neurons and perivascular astrocytes in the hippocampus of experimental temporal lobe epilepsy. Epilepsia 50:654–663.

Kim JE, Ryu HJ, Yeo SI, Seo CH, Lee BC, Choi IG, Kim DS, Kang TC (2009b) Differential expressions of aquaporin subtypes in astroglia in the hippocampus of chronic epileptic rats. Neuroscience 163:781–789.

Kim SJ, Cho SJ, Jang JM, Shin J, Park PW, Lee YJ, Cho IH, Choi JE, Lee HJ (2010) Interaction between brain-derived neurotrophic factor Val66Met polymorphism and recent negative stressor in harm avoidance. Neuropsychobiology 61:19–26.

Kinney GG, Patino P, Mermet-Bouvier Y, Starrett JE Jr, Gribkoff VK (1999) Cognition-enhancing drugs increase stimulated hippocampal theta rhythm amplitude in the urethane-anesthetized rat. J Pharmacol Exp Ther 291:99–106.

Lanzenberger RR, Mitterhauser M, Spindelegger C, Wadsak W, Klein N, Mien LK, Holik A, Attarbaschi T, Mossaheb N, Sacher J, Geiss-Granadia T, Kletter K, Kasper S, Tauscher J (2007) Reduced serotonin-1A receptor binding in social anxiety disorder. Biol Psychiatry 61:1081–1089.

Leung LS (1998) Generation of theta and gamma rhythms in the hippocampus. Neurosci Biobehav Rev 22:275–290.

Levey A, Lah J, Goldstein F, Steenland K, Bliwise D (2006) Mild cognitive impairment: an opportunity to identify patients at high risk for progression to Alzheimer's disease. Clin Ther 28:991–1001.

Mariani E, Monastero R, Mecocci P (2007) Mild cognitive impairment: a systematic review. J Alzheimers Dis 12:23–35.

McNaughton N, Kocsis B, Hajós M (2007) Elicited hippocampal theta rhythm: a screen for anxiolytic and procognitive drugs through changes in hippocampal function? Behav Pharmacol 118:329–346.

Mitchell DJ, McNaughton N, Flanagan D, Kirk IJ (2008) Frontal-midline theta from the perspective of hippocampal "theta." Prog Neurobiol 86:156–185.

Miyata M, Kashiwadani H, Fukaya M, Hayashi T, Wu D, Suzuki T, Watanabe M, Kawakami Y (2003) Role of thalamic phospholipase Cβ4 mediated by metabotropic glutamate receptor type 1 in inflammatory pain. J Neurosci 23:8098–8108.

Mizuki Y, Suetsugi M, Imai T, Kai S, Kajimura N, Yamada M (1989) A physiological marker for assessing anxiety level in humans: frontal midline theta activity. Jpn J Psychiatry Neurol 43:619–626.

Nakamura M, Sato K, Fukaya M, Araishi K, Aiba A, Kano M, Watanabe M (2004) Signaling complex formation of phospholipase Cbeta4 with metabotropic glutamate receptor type 1alpha and 1,4,5-trisphosphate receptor at the perisynapse and endoplasmic reticulum in the mouse brain. Eur J Neurosci 20:2929–2944.

Narushima M, Uchigashima M, Fukaya M, Matsui M, Manabe T, Hashimoto K, Watanabe M, Kano M (2007) Tonic enhancement of endocannabinoid-mediated retrograde suppression of inhibition by cholinergic interneuron activity in the striatum. J Neurosci 27:496–506.

Nutt DJ (2005) Overview of diagnosis and drug treatments of anxiety disorders. CNS Spectr 10:49–56.

Park D, Lee S, Jun K, Hong YM, Kim DY, Kim YI, Shin HS (2003) Translation of clock rhythmicity into neural firing in suprachiasmatic nucleus requires mGluR-PLCbeta4 signaling. Nat Neurosci 6:337–338.

Parks CL, Robinson PS, Sibille E, Shenk T, Toth M (1998) Increased anxiety of mice lacking the serotonin1A receptor. Proc Natl Acad Sci U S A 95:10734–10739.

Porter VR, Buxton WG, Fairbanks LA, Strickland T, O'Connor SM, Rosenberg-Thompson S, Cummings JL (2003) Frequency and characteristics of anxiety among patients with Alzheimer's disease and related dementias. J Neuropsychiatry Clin Neurosci 15:180–186.

Ramboz S, Oosting R, Amara DA, Kung HF, Blier P, Mendelsohn M, Mann JJ, Brunner D, Hen R (1998) Serotonin receptor 1A knockout: an animal model of anxiety-related disorder. Proc Natl Acad Sci U S A 95:14476–14481.

Santin LJ, Bilbao A, Pedraza C, Matas-Rico E, López-Barroso D, Castilla-Ortega E, Sánchez-López J, Riquelme R, Varela-Nieto I, de la Villa P, Suardíaz M, Chun J, De Fonseca FR, Estivill-Torrús G (2009) Behavioral phenotype of maLPA-null mice: increased anxiety-like behavior and spatial memory deficits. Genes Brain Behav 8:772–784.

Shin J (2002) A unifying theory on the relationship between spike trains, EEG, and ERP based on the noise shaping/predictive neural coding hypothesis. Biosystems 67:245–257.

Shin J (2009) Passive rotation-induced theta rhythm and orientation homeostasis response. Synapse, in press.

Shin J, Talnov A (2001) A single trial analysis of hippocampal theta frequency during nonsteady wheel running in rats. Brain Res 897:217–221.

Shin J, Koch C, Douglas R (1999) Adaptive neural coding dependent on the

time-varying statistics of the somatic input current. Neural Comput 11:1893–1913.

Shin J, Kim D, Bianchi R, Wong RK, Shin HS (2005) Genetic dissection of theta rhythm heterogeneity in mice. Proc Natl Acad Sci U S A 102:18165–18170.

Sienkiewicz-Jarosz H, Członkowska AI, Siemiatkowski M, Maciejak P, Szyndler J, Płaźnik A (2000) The effects of physostigmine and cholinergic receptor ligands on novelty-induced neophobia. J Neural Transm 107: 1403–1412.

Smythe JW, Colom LV, Bland BH (1992) The extrinsic modulation of hippocampal theta depends on the coactivation of cholinergic and GABAergic medial septal inputs. Neurosci Biobehav Rev 16:289–308.

Suetsugi M, Mizuki Y, Ushijima I, Kobayashi T, Tsuchiya K, Aoki T, Watanabe Y (2000) Appearance of frontal midline theta activity in patients with generalized anxiety disorder. Neuropsychobiology 41:108–112.

Tanaka J, Nakagawa S, Kushiya E, Yamasaki M, Fukaya M, Iwanaga T, Simon MI, Sakimura K, Kano M, Watanabe M (2000) Gq protein alpha subunits Galphaq and Galpha11 are localized at postsynaptic extra-junctional membrane of cerebellar Purkinje cells and hippocampal pyramidal cells. Eur J Neurosci 12:781–792.

Toth M (2003) 5-HT1A receptor knockout mouse as a genetic model of anxiety. Eur J Pharmacol 463:177–184.

Treit D, Fundytus M (1988) Thigmotaxis as a test for anxiolytic activity in rats. Pharmacol Biochem Behav 31:959–962.

Treit D, Menard J (1997) Dissociations among the anxiolytic effects of septal, hippocampal, and amygdaloid lesions. Behav Neurosci 111:653–658.

Van Dam D, Abramowski D, Staufenbiel M, De Deyn PP (2005) Symptomatic effect of donepezil, rivastigmine, galantamine and memantine on cognitive deficits in the APP23 model. Psychopharmacology (Berl) 180: 177–190.

Watanabe M, Nakamura M, Sato K, Kano M, Simon MI, Inoue Y (1998) Patterns of expression for the mRNA corresponding to the four isoforms of phospholipase Cbeta in mouse brain. Eur J Neurosci 10:2016–2025.

Welch JM, Lu J, Rodriguiz RM, Trotta NC, Peca J, Ding JD, Feliciano C, Chen M, Adams JP, Luo J, Dudek SM, Weinberg RJ, Calakos N, Wetsel WC, Feng G (2007) Cortico-striatal synaptic defects and OCD-like behaviours in Sapap3-mutant mice. Nature 448:894–900.

Wu M, Hajszan T, Leranth C, Alreja M (2003a) Nicotine recruits a local glutamatergic circuit to excite septohippocampal GABAergic neurons. Eur J Neurosci 18:1155–1168.

Wu M, Newton SS, Atkins JB, Xu C, Duman RS, Alreja M (2003b) Acetylcholinesterase inhibitors activate septohippocampal GABAergic neurons via muscarinic but not nicotinic receptors. J Pharmacol Exp Ther 307: 535–543.

Wu M, Hajszan T, Xu C, Leranth C, Alreja M (2004) Group I metabotropic glutamate receptor activation produces a direct excitation of identified septohippocampal cholinergic neurons. J Neurophysiol 92:1216–1225.

Wulff P, Ponomarenko AA, Bartos M, Korotkova TM, Fuchs EC, Bähner F, Both M, Tort AB, Kopell NJ, Wisden W, Monyer H (2009) Hippocampal theta rhythm and its coupling with gamma oscillations require fast inhibition onto parvalbumin-positive interneurons. Proc Natl Acad Sci U S A 106:3561–3566.

Yamada K, Fukaya M, Shimizu H, Sakimura K, Watanabe M (2001) NMDA receptor subunits GluRepsilon1, GluRepsilon3 and GluRzeta1 are enriched at the mossy fibre-granule cell synapse in the adult mouse cerebellum. Eur J Neurosci 13:2025–2036.